A Nd_6 Molecular Butterfly: An Unique All-in-One Material for SMM, MCE and Maiden Photosensitized Opto-electronic Device Fabrication.

Krishna Sundar Das, Sayan Saha, Baisakhi Paul, Amit Adhikary, Shruti Moorthy, Sukhen Bala, Sohel Akhtar, Pradipta Ghosh, Saurabh Kumar Singh,* Partha Pratim Roy,* Raju Mondal*

Supporting Information

Table S1. Crystallographic data and refinement parameters of **Nd_6**.

Empirical formula	$C_{83}H_{81}N_{41}Nd_6O_{39}$
Formula weight	3142.32
Temperature/K	120(2)
Crystal system	monoclinic
Space group	C 2/c
a/Å	25.0768(12)
b/Å	17.7222(8)
c/Å	30.3551(15)
α/°	90
β/°	106.586(2)
γ/°	90
Volume/Å^3	12929.0(11)
Z	4
no. of rflns collected	77497
no. of unique rflns	14915
no. of obsd rflns (I > 2σ(I))	9525
R1 (I > 2σ(I))	0.0836
wR2 (> 2σ(I))	0.2226
CCDC no.	2085378

Table S2. Selected bond lengths and bond angles

Nd_6 complex		
Bond lengths	Bond angles	
Nd1 O1S 2.424(4)	O1S Nd1 O2 117.6(2)	N6 Nd3 O1SD 88.1(3)
Nd1 O2 2.482(6)	O1S Nd1 O1SC 76.9(2)	O1 Nd3 C1SD 99.7(3)
Nd1 O1SC 2.489(6)	O2 Nd1 O1SC 63.85(19)	O2 Nd3 C1SD 96.2(3)
Nd1 O1A 2.490(7)	O1S Nd1 O1A 117.4(2)	O2S Nd3 C1SD 150.1(3)
Nd1 O2SA 2.511(6)	O2 Nd1 O1A 125.0(2)	O2SD Nd3 C1SD 24.9(3)
Nd1 O2SB 2.544(6)	O1SC Nd1 O1A 130.8(2)	N9 Nd3 C1SD 101.4(3)
Nd1 O1SA 2.548(6)	O1S Nd1 O2SA 74.9(2)	O1SC Nd3 C1SD 69.8(3)
Nd1 N11 2.585(8)	O2 Nd1 O2SA 132.0(2)	N5 Nd3 C1SD 78.9(4)
Nd1 N3A 2.594(7)	O1SC Nd1 O2SA 151.8(2)	O1SB Nd3 C1SD 139.1(3)

Nd2 O1S 2.453(9)	O1A Nd1 O2SA 64.3(2)	N6 Nd3 C1SD 82.1(3)
Nd2 O1 2.457(6)	O1S Nd1 O2SB 72.51(14)	O1SD Nd3 C1SD 24.0(3)
Nd2 O1 2.457(6)	O2 Nd1 O2SB 69.31(19)	O1A Nd4 O1A 122.0(3)
Nd2 O1SB 2.503(6)	O1SC Nd1 O2SB 100.1(2)	O1A Nd4 O1SS 118.3(4)
Nd2 O1SB 2.503(6)	O1A Nd1 O2SB 128.9(2)	O1A Nd4 O1SS 76.3(3)
Nd2 N3 2.557(8)	O2SA Nd1 O2SB 72.03(19)	O1A Nd4 O1SS 76.3(3)
Nd2 N3 2.557(8)	O1S Nd1 O1SA 72.88(14)	O1A Nd4 O1SS 118.3(4)
Nd2 O2SC 2.573(6)	O2 Nd1 O1SA 128.56(19)	O1SS Nd4 O1SS 151.7(5)
Nd2 O2SC 2.573(6)	O1SC Nd1 O1SA 71.4(2)	O1A Nd4 O3SS 74.3(4)
Nd3 O1 2.429(6)	O1A Nd1 O1SA 69.6(2)	O1A Nd4 O3SS 117.3(4)
Nd3 O2 2.499(6)	O2SA Nd1 O1SA 99.4(2)	O1SS Nd4 O3SS 48.8(4)
Nd3 O2S 2.514(8)	O2SB Nd1 O1SA 145.39(18)	O1SS Nd4 O3SS 124.4(5)
Nd3 O2SD 2.518(7)	O1S Nd1 N11 139.74(18)	O1A Nd4 O3SS 117.3(4)
Nd3 N9 2.558(7)	O2 Nd1 N11 64.2(2)	O1A Nd4 O3SS 74.3(4)
Nd3 O1SC 2.586(6)	O1SC Nd1 N11 126.8(2)	O1SS Nd4 O3SS 124.4(5)
Nd3 N5 2.597(8)	O1A Nd1 N11 74.2(2)	O1SS Nd4 O3SS 48.8(4)
Nd3 O1SB 2.599(5)	O2SA Nd1 N11 77.4(2)	O3SS Nd4 O3SS 157.7(7)
Nd3 N6 2.709(8)	O2SB Nd1 N11 71.5(2)	O1A Nd4 N5A 60.0(3)
Nd3 O1SD 2.724(9)	O1SA Nd1 N11 140.9(2)	O1A Nd4 N5A 172.7(4)
Nd3 C1SD 2.961(13)	O1S Nd1 N3A 143.01(18)	O1SS Nd4 N5A 96.6(5)
Nd4 O1A 2.486(6)	O2 Nd1 N3A 73.3(2)	O1SS Nd4 N5A 68.8(5)
Nd4 O1A 2.486(6)	O1SC Nd1 N3A 77.9(2)	O3SS Nd4 N5A 55.7(5)
Nd4 O1SS 2.493(10)	O1A Nd1 N3A 63.4(2)	O3SS Nd4 N5A 111.6(5)
Nd4 O1SS 2.494(10)	O2SA Nd1 N3A 126.2(2)	O1A Nd4 N5A 172.7(4)
Nd4 O3SS 2.560(13)	O2SB Nd1 N3A 138.8(2)	O1A Nd4 N5A 60.0(3)
Nd4 O3SS 2.560(13)	O1SA Nd1 N3A 73.7(2)	O1SS Nd4 N5A 68.8(5)
Nd4 N5A 2.605(11)	N11 Nd1 N3A 77.3(3)	O1SS Nd4 N5A 96.6(5)
Nd4 N5A 2.605(11)	O1S Nd2 O1 118.65(16)	O3SS Nd4 N5A 111.6(5)
Nd4 N6A 2.607(12)	O1S Nd2 O1 118.65(16)	O3SS Nd4 N5A 55.7(5)
Nd4 O2SA 2.614(6)	O1 Nd2 O1 122.7(3)	N5A Nd4 N5A 119.1(5)
Nd4 O2SA 2.614(6)	O1S Nd2 O1SB 77.17(14)	O1A Nd4 N6A 119.02(15)
Nd4 N1SS 2.89(2)	O1 Nd2 O1SB 130.4(2)	O1SS Nd4 N6A 75.8(2)
	O1 Nd2 O1SB 64.2(2)	O3SS Nd4 N6A 78.9(3)
	O1S Nd2 O1SB 77.17(14)	N5A Nd4 N6A 59.6(2)
	O1 Nd2 O1SB 64.2(2)	O1A Nd4 O2SA 69.5(2)
	O1 Nd2 O1SB 130.4(2)	O1A Nd4 O2SA 62.9(2)

	O1SB Nd2 O1SB 154.3(3) O1S Nd2 N3 137.80(19) O1 Nd2 N3 63.5(2) O1 Nd2 N3 74.7(3) O1SB Nd2 N3 74.2(2) O1SB Nd2 N3 126.9(2) O1S Nd2 N3 137.80(19) O1 Nd2 N3 74.7(2) O1 Nd2 N3 63.5(2) O1SB Nd2 N3 126.9(2) O1SB Nd2 N3 74.2(2) N3 Nd2 N3 84.4(4) O1S Nd2 O2SC 72.44(15) O1 Nd2 O2SC 129.1(2) O1 Nd2 O2SC 70.0(2) O1SB Nd2 O2SC 100.14(19) O1SB Nd2 O2SC 71.93(18) N3 Nd2 O2SC 142.8(2) N3 Nd2 O2SC 69.6(2) O1S Nd2 O2SC 72.44(15) O1 Nd2 O2SC 70.0(2) O1 Nd2 O2SC 129.1(2) O1SB Nd2 O2SC 71.93(18) O1SB Nd2 O2SC 100.14(19) N3 Nd2 O2SC 69.6(2) N3 Nd2 O2SC 142.8(2) O2SC Nd2 O2SC 144.9(3) O1 Nd3 O2 121.4(2) O1 Nd3 O2S 83.5(2) O2 Nd3 O2S 107.5(2) O1 Nd3 O2SD 123.4(2) O2 Nd3 O2SD 77.1(2) O2S Nd3 O2SD 146.4(2) O1 Nd3 N9 158.4(3) O2 Nd3 N9 60.6(2) O2S Nd3 N9 76.0(2)	O1SS Nd4 O2SA 72.1(3) O1SS Nd4 O2SA 135.6(3) O3SS Nd4 O2SA 72.2(4) O3SS Nd4 O2SA 128.8(4) N5A Nd4 O2SA 113.8(3) N5A Nd4 O2SA 116.0(3) N6A Nd4 O2SA 146.19(14) O1A Nd4 O2SA 62.9(2) O1A Nd4 O2SA 69.5(2) O1SS Nd4 O2SA 135.6(3) O1SS Nd4 O2SA 72.1(3) O3SS Nd4 O2SA 128.8(4) O3SS Nd4 O2SA 72.2(4) N5A Nd4 O2SA 116.0(3) N5A Nd4 O2SA 113.8(3) N6A Nd4 O2SA 146.18(14) O2SA Nd4 O2SA 67.6(3) O1A Nd4 N1SS 93.3(3) O1A Nd4 N1SS 97.9(3) O1SS Nd4 N1SS 146.1(4) O1SS Nd4 N1SS 21.8(3) O3SS Nd4 N1SS 144.3(4) O3SS Nd4 N1SS 27.2(4) N5A Nd4 N1SS 88.9(5) N5A Nd4 N1SS 79.4(5) N6A Nd4 N1SS 78.4(3) O2SA Nd4 N1SS 135.3(4) O2SA Nd4 N1SS 67.8(4) Nd1 O1S Nd1 121.7(4) Nd1 O1S Nd2 119.14(18) Nd1 O1S Nd2 119.14(18) Nd3 O2S H2SA 109.5 O1SS N1SS Nd4 58.1(11) O3SS N1SS Nd4 62.2(10) O2SS N1SS Nd4 166.4(12) N1SS O1SS Nd4 100.2(12)

	O2SD Nd3 N9 78.1(2) O1 Nd3 O1SC 71.4(2) O2 Nd3 O1SC 62.24(18) O2S Nd3 O1SC 137.5(2) O2SD Nd3 O1SC 74.8(2) N9 Nd3 O1SC 120.5(2) O1 Nd3 N5 61.2(2) O2 Nd3 N5 174.9(3) O2S Nd3 N5 76.8(3) O2SD Nd3 N5 97.8(3) N9 Nd3 N5 119.0(2) O1SC Nd3 N5 116.5(2) O1 Nd3 O1SB 63.1(2) O2 Nd3 O1SB 68.22(19) O2S Nd3 O1SB 68.7(2) O2SD Nd3 O1SB 138.6(2) N9 Nd3 O1SB 102.5(2) O1SC Nd3 O1SB 69.49(19) N5 Nd3 O1SB 116.3(2) O1 Nd3 N6 118.4(2) O2 Nd3 N6 119.5(2) O2S Nd3 N6 70.6(3) O2SD Nd3 N6 78.3(2) N9 Nd3 N6 60.7(2) O1SC Nd3 N6 151.8(2) N5 Nd3 N6 59.0(3) O1SB Nd3 N6 138.7(2) O1 Nd3 O1SD 76.5(2) O2 Nd3 O1SD 113.4(2) O2S Nd3 O1SD 139.0(3) O2SD Nd3 O1SD 48.9(2) N9 Nd3 O1SD 123.9(2) O1SC Nd3 O1SD 67.7(2) N5 Nd3 O1SD 62.3(3)	N1SS O3SS Nd4 90.5(11) C1SA O1SA Nd1 115.5(6) C1SA O2SA Nd1 125.4(5) C1SA O2SA Nd4 122.7(5) Nd1 O2SA Nd4 109.7(2) C1SB O1SB Nd2 122.3(5) C1SB O1SB Nd3 126.9(5) Nd2 O1SB Nd3 108.1(2) C1SB O2SB Nd1 115.9(5) C1SC O1SC Nd1 121.7(5) C1SC O1SC Nd3 124.2(5) Nd1 O1SC Nd3 111.3(2) C1SC O2SC Nd2 116.5(6) C1SD O1SD Nd3 89.1(8) C1SD O2SD Nd3 97.7(7) O1SD C1SD Nd3 66.9(7) O2SD C1SD Nd3 57.4(6) Nd3 C1SD H1SB 174.8 C9 O1 Nd3 119.2(6) C9 O1 Nd2 124.4(6) Nd3 O1 Nd2 115.5(3) C19 O2 Nd1 122.6(5) C19 O2 Nd3 120.4(5) Nd1 O2 Nd3 114.6(2) C8 N3 Nd2 120.1(6) N2 N3 Nd2 134.1(6) C10 N5 Nd3 125.3(7) N4 N5 Nd3 118.4(6) C12 N6 Nd3 120.9(7) C16 N6 Nd3 120.3(6) C17 N9 Nd3 126.6(6) N10 N9 Nd3 121.2(5) N12 N11 Nd1 138.5(6) C20 N11 Nd1 117.3(6)

Figure S1. Image of the single crystals.

PXRD Data:

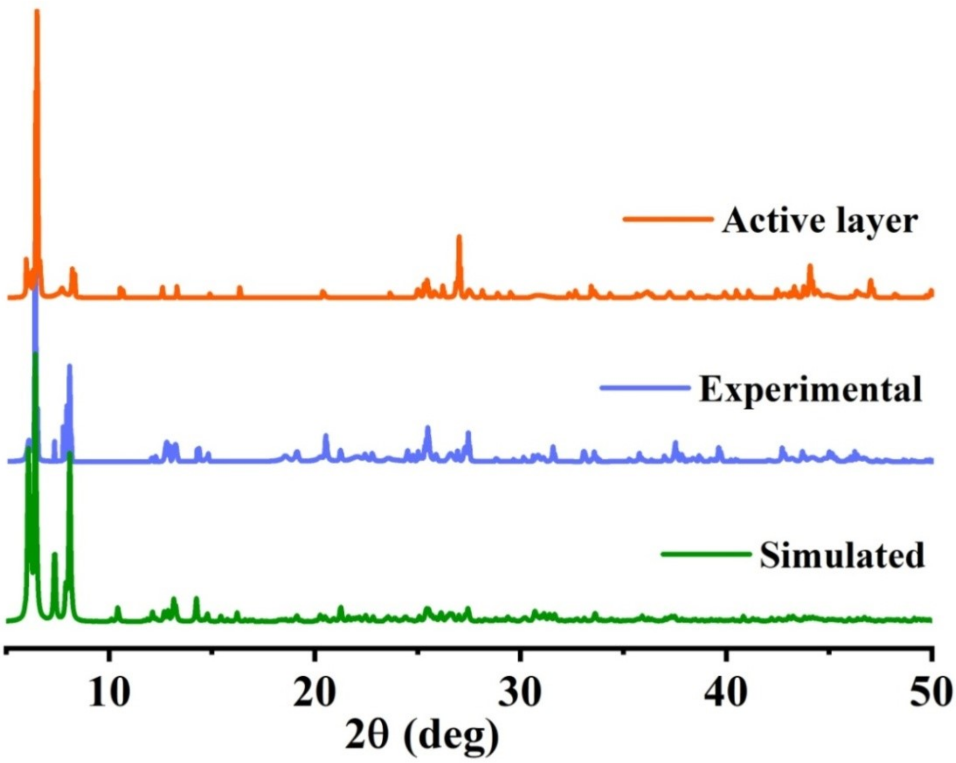

Figure S2. PXRD data of the 'big' single crystal showing its phase purity.

Characterization Data:

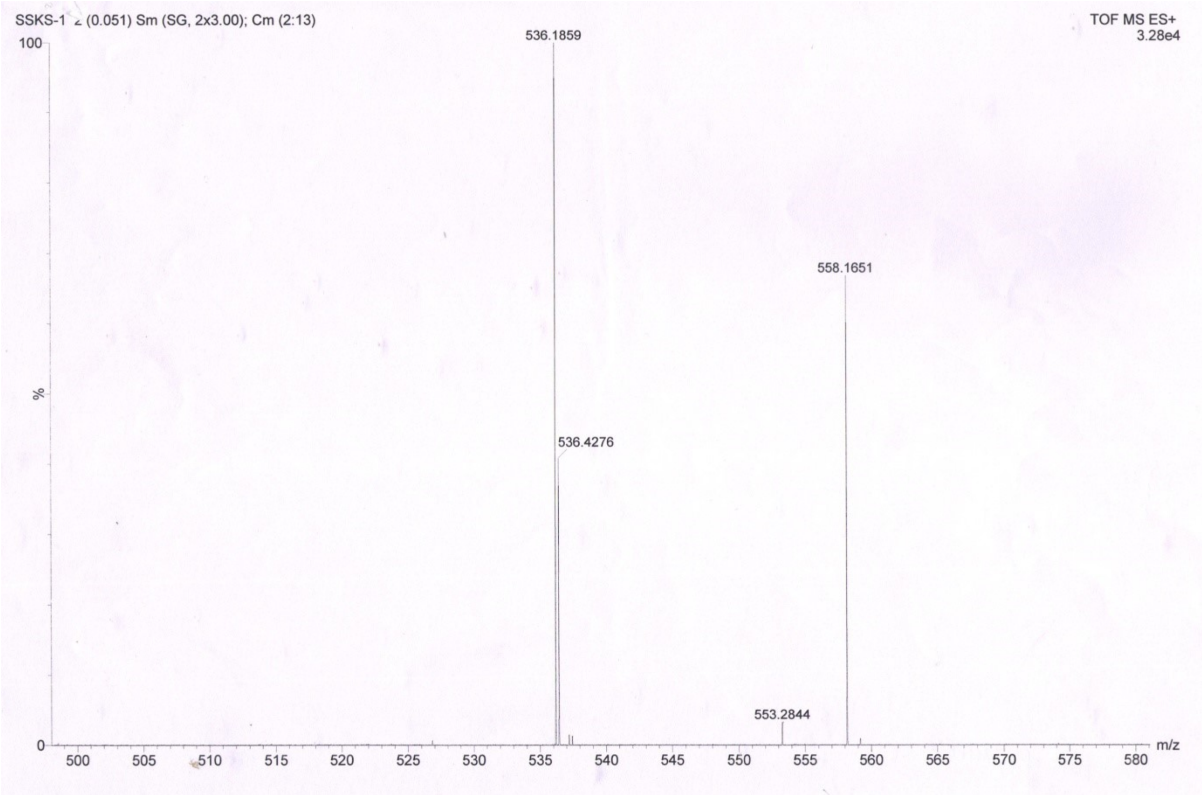

Figure S3. HRMS of BMPC ligand.

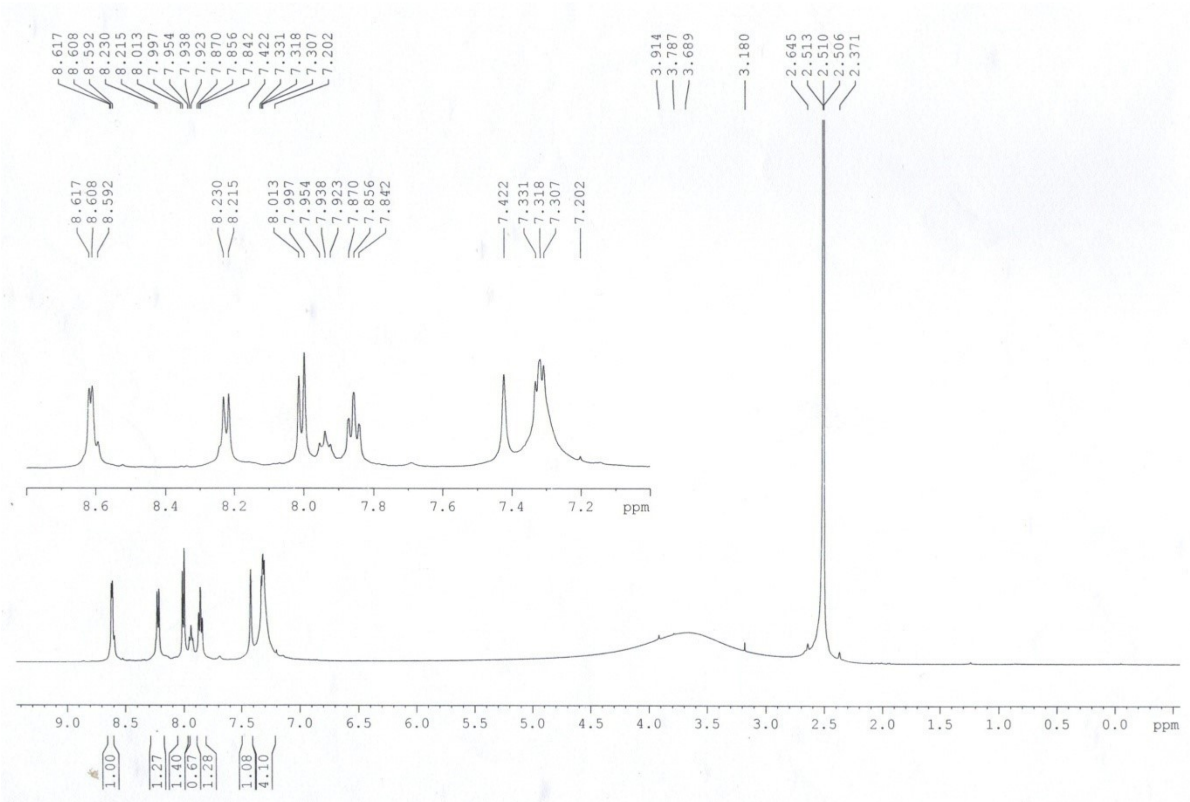

Figure S4. [1]HNMR of BMPC ligand.

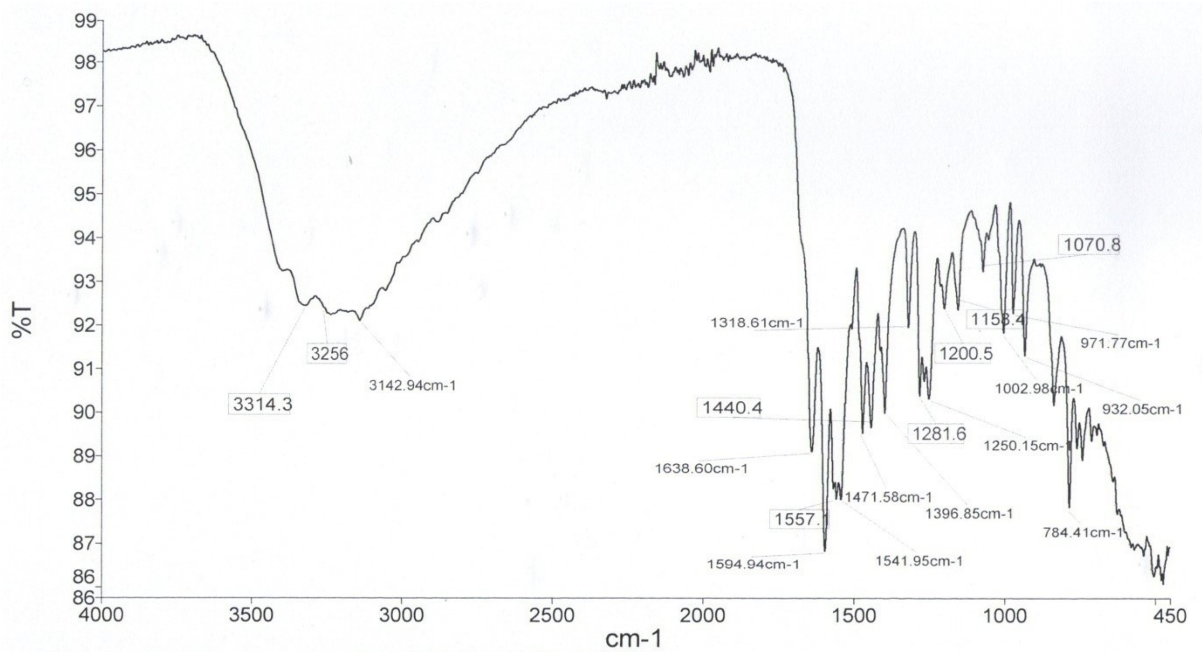

Figure S5. IR data of BMPC ligand.

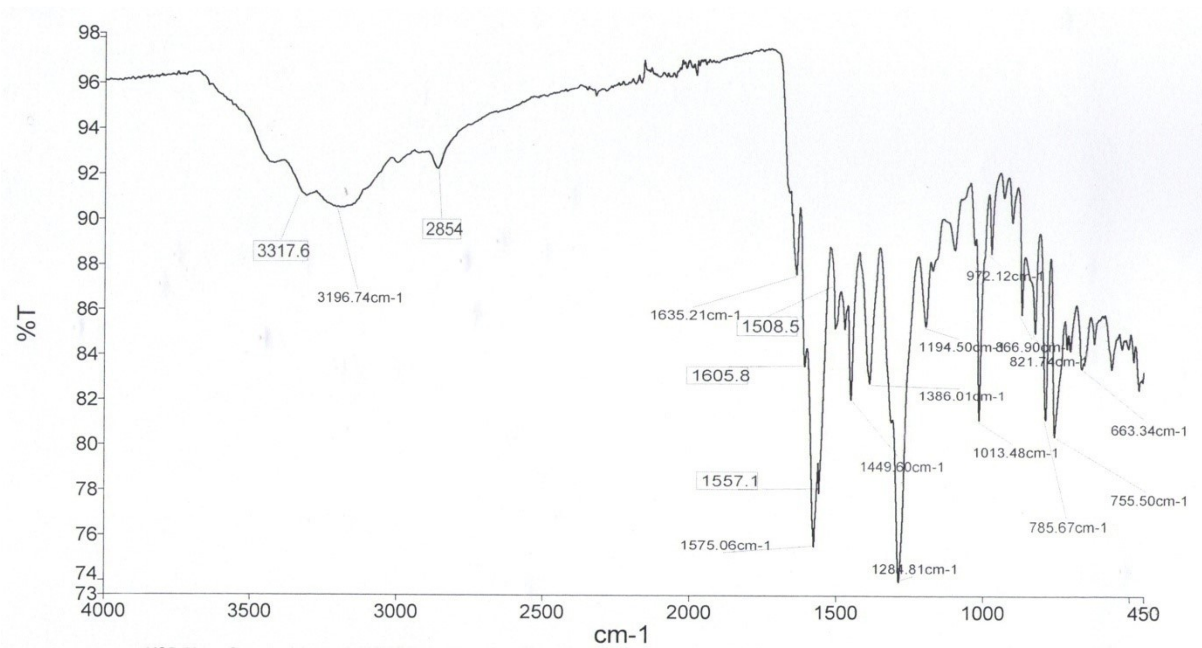

Figure S6. IR data of Nd6 compound.

Ligation of Nd centers:

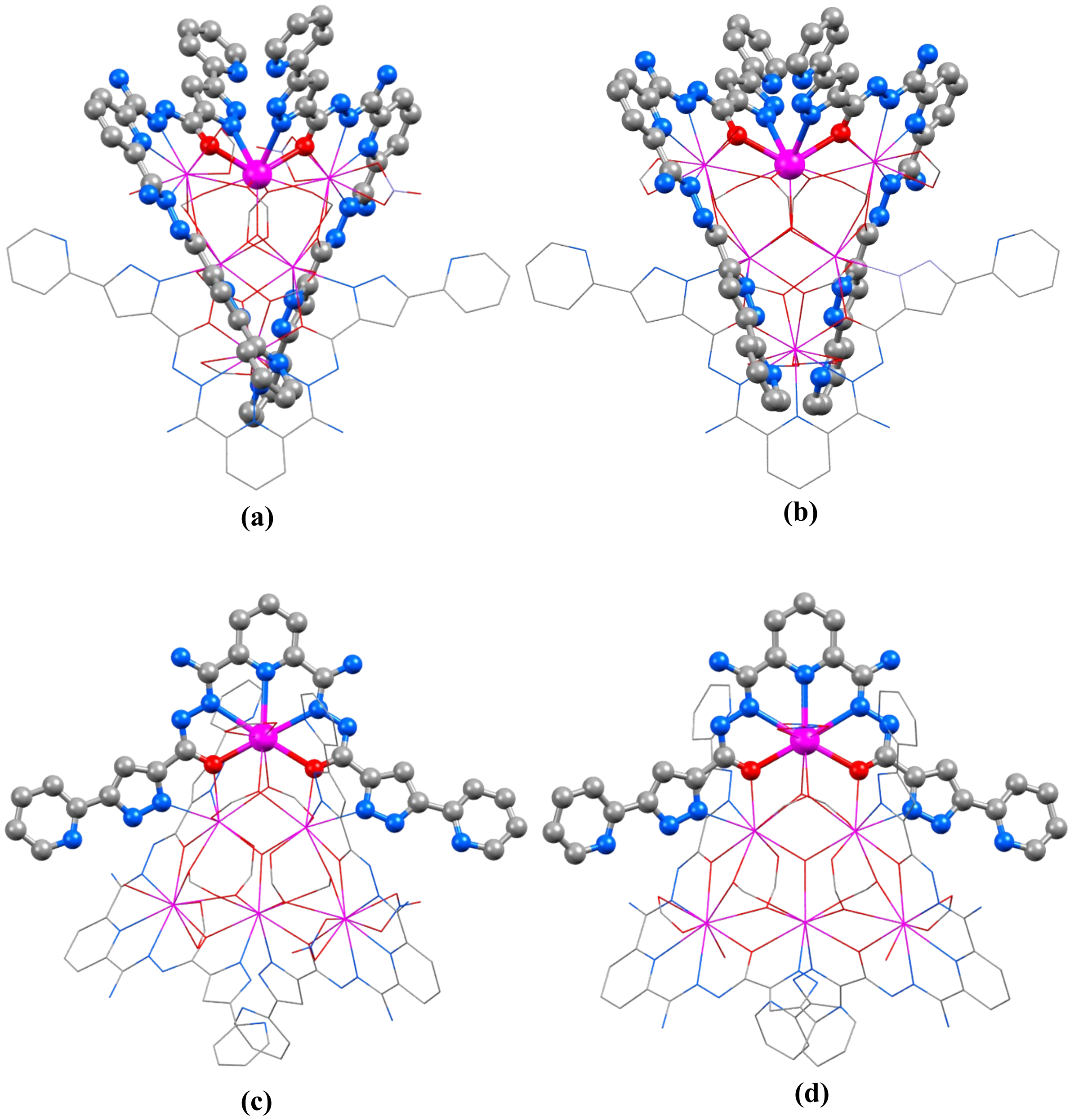

Figure S7. Ligation to different metal centers such as (a)Nd1, (b)Nd2, (c)Nd3 and (d)Nd4.

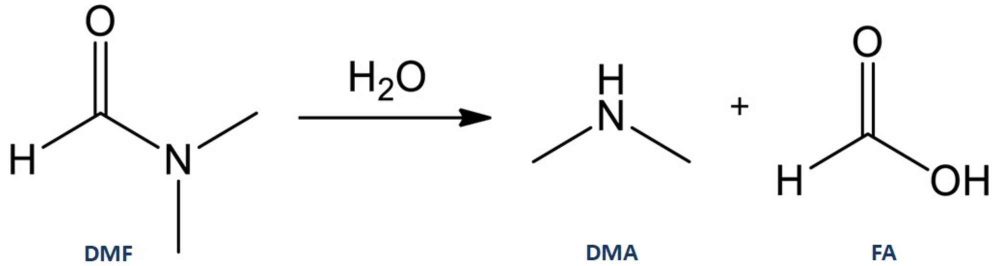

Scheme S1. Generation of formic acid.

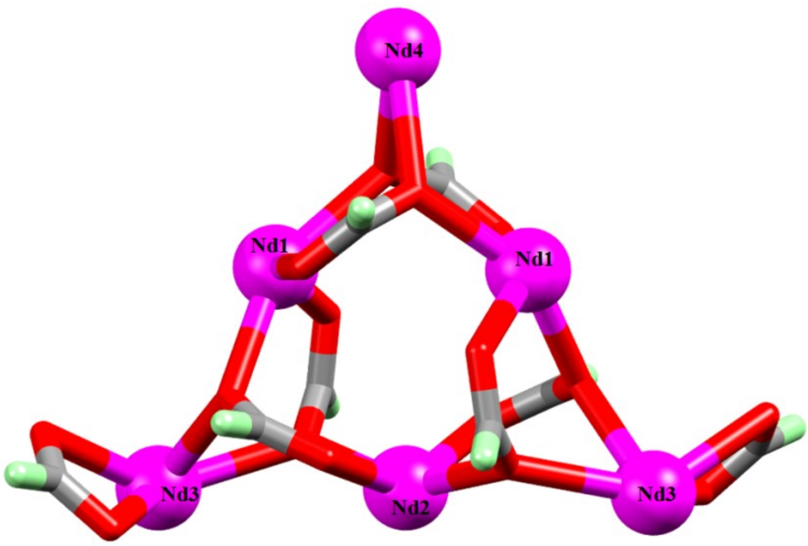

Figure S8. Formate binding to the Nd_6 core.

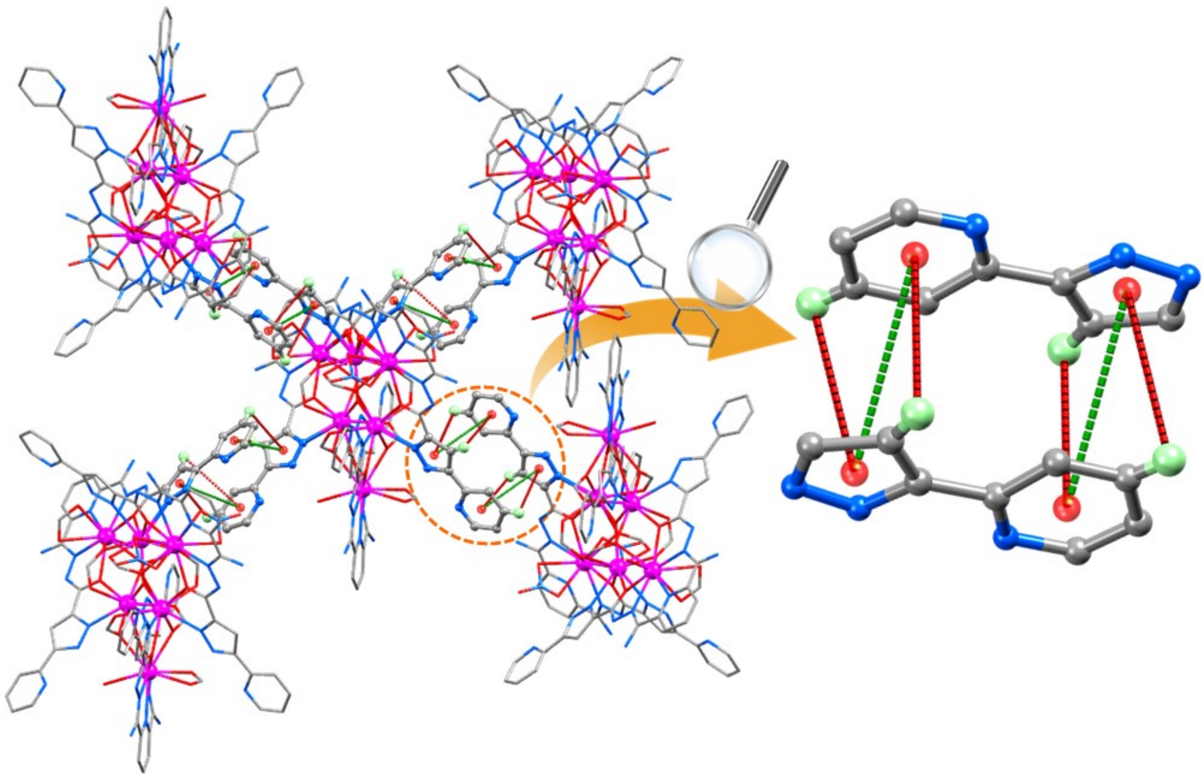

Figure S9. Extensive supramolecular interactions (π–π and C-H–π) with the adjacent Nd_6 molecules.

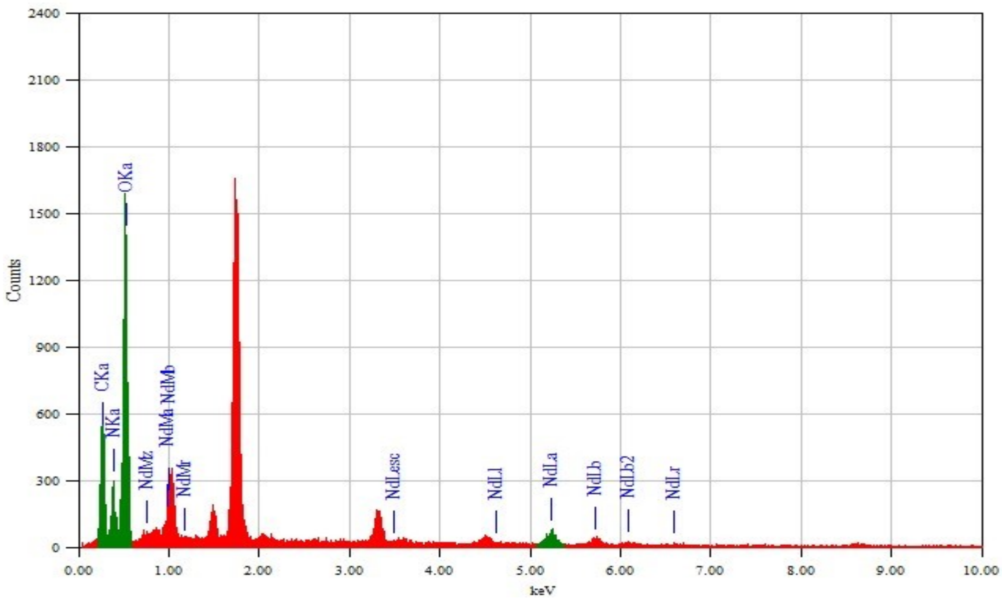

Figure S10. EDX data from FESEM study.

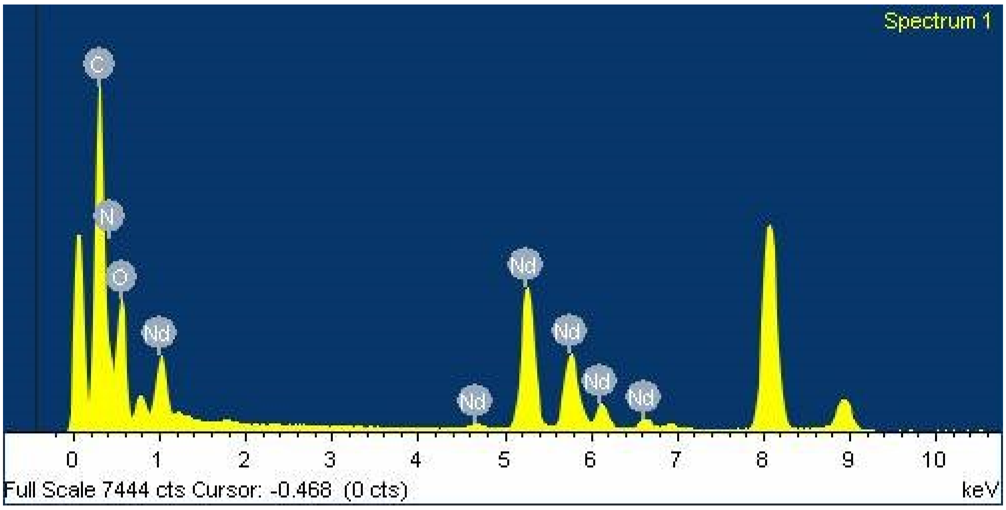

Figure S11. EDX data from FEGTEM study.

Table S3. Percentage of elements from FEGTEM study.

Element	Weight%	Atomic%
C	37.18	65.93
N	8.43	12.82
O	11.17	14.86
Nd	43.22	6.38

Table S4. Nd(III) geometry analysis by using Continuous Shape Measurements (CShM).[1,2]

Nd1	EP-9	OPY-9	HBPY-9	JTC-9	JCCU-9	CCU-9	JCSAPR-9
	(D_{9h})	(C_{8v})	(D_{7h})	(C_{3v})	(C_{4v})	(C_{4v})	(C_{4v})
	36.981	22.357	18.648	16.470	10.932	9.542	2.359
	JTCTPR-9	TCTPR-9	JTDIC-9	HH-9	MFF-9		
	(D_{3h})	(D_{3h})	(C_{3v})	(C_{2v})	(C_s)		
	3.317	**0.999**	11.301	10.096	1.431		
Nd2	EP-9	OPY-9	HBPY-9	JTC-9	JCCU-9	CCU-9	JCSAPR-9
	(D_{9h})	(C_{8v})	(D_{7h})	(C_{3v})	(C_{4v})	(C_{4v})	(C_{4v})
	36.161	21.241	19.251	16.736	11.299	9.839	2.561
	CSAPR-9	JTCTPR-9	TCTPR-9	JTDIC-9	HH-9	MFF-9	
	(C_{4v})	(D_{3h})	(D_{3h})	(C_{3v})	(C_{2v})	(C_s)	
	1.370	3.500	**0.749**	10.273	10.754	1.890	
Nd3	DP-10	EPY-10	OBPY-10	PPR-10	PAPR-10	JBCCU-10	JBCSAPR-
	(D_{10h})	(C_{9v})	(D_{8h})	(D_{5h})	(D_{5d})	(D_{4h})	(D_{4d})
	36.135	24.813	16.149	11.462	9.889	11.981	5.051
	JMBIC-10	JATDI-10	JSPC-10	SDD-10	TD-10	HD-10	
	(C_{2v})	(C_{3v})	(C_{2v})	(D_2)	(C_{2v})	(D_{4h})	
	5.414	17.639	4.005	3.343	**3.049**	9.091	
Nd4	HP-11	DPY-11	EBPY-11	JCPPR-11	JCPAPR-11	JAPPR-11	
	(D_{11h})	(C_{10v})	(D_{9h})	(C_{5v})	(C_{5v})	(C_{2v})	
	36.963	25.182	17.147	8.851	**3.835**	12.668	
	JASPC-11						
	(C_s)						
	6.185						

Where, **EP-9**: Enneagon, **OPY-9**: Octagonal pyramid, **HBPY-9**: Heptagonal bipyramid **JTC-9**: Johnson triangular cupola J3, **JCCU-9**: Capped cube J8, **CCU-9**: Spherical-relaxed capped cube, **JCSAPR-9**: Capped square antiprism J10, **JTCTPR-9**: Tricapped trigonal prism J51, **TCTPR-9**: Spherical tricapped trigonal prism, **JTDIC-9**: Tridiminished icosahedron J63, **HH-9**: Hula-hoop, **MFF-9**: Muffin, **DP-10**: Decagon, **EPY-10**: Enneagonal pyramid, **OBPY-10**: Octagonal bipyramid, **PPR-10**: Pentagonal prism, **PAPR-10**: Pentagonal antiprism, **JBCCU-10**: Bicapped cube J15, **JBCSAPR-10**: Bicapped square antiprism J17, **JMBIC-10**: Metabidiminished icosahedron J62, **JATDI-10**: Augmented tridiminished icosahedron J64, **JSPC-10**: Sphenocorona J87, **SDD-10**: Staggered Dodecahedron (2:6:2), **TD-10**: Tetradecahedron (2:6:2), HD-10: Hexadecahedron (2:6:2) or (1:4:4:1), HP-11: Hendecagon, **DPY-11**: Decagonal pyramid, **EBPY-11**: Enneagonal bipyramid, **JCPPR-11**: Capped pentagonal prism J9, **JCPAPR-11**: Capped pentagonal antiprism J11, **JAPPR-11**: Augmented pentagonal prism J52, **JASPC-11**: Augmented sphenocorona J87.

Table S5. Plausible Nd(III) geometries on the basis of CShM.

Nd1		Nd2	
C. N.- 9 Symm.- D_{3h} Geom.- Spherical tricapped trigonal prism	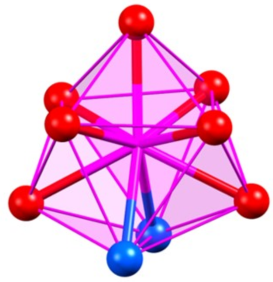	C. N.- 9 Symm.- D_{3h} Geom.- Spherical tricapped trigonal prism	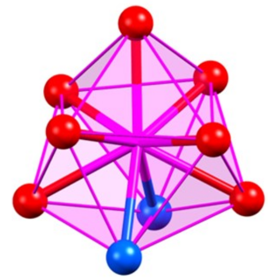
Nd3		**Nd4**	
C. N.- 10 Symm.- C_{2v} Geom.- Tetradecahedron	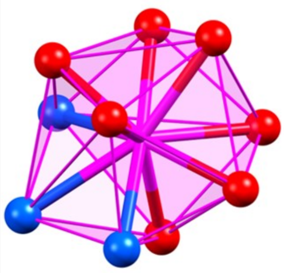	C. N.- 11 Symm.- C_{2v} Geom.- Capped pentagonal antiprism	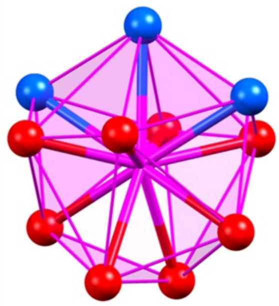

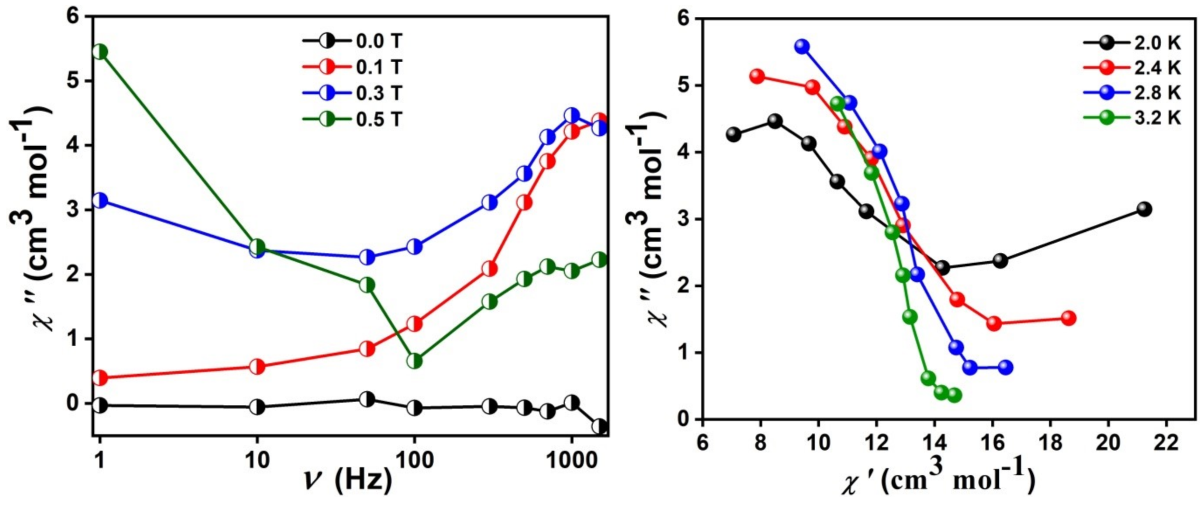

(a) (b)

Figure S12. AC data sowing (a) out of phase magnetic succeptibility plot at different DC fields and (b) cole-cole plot.

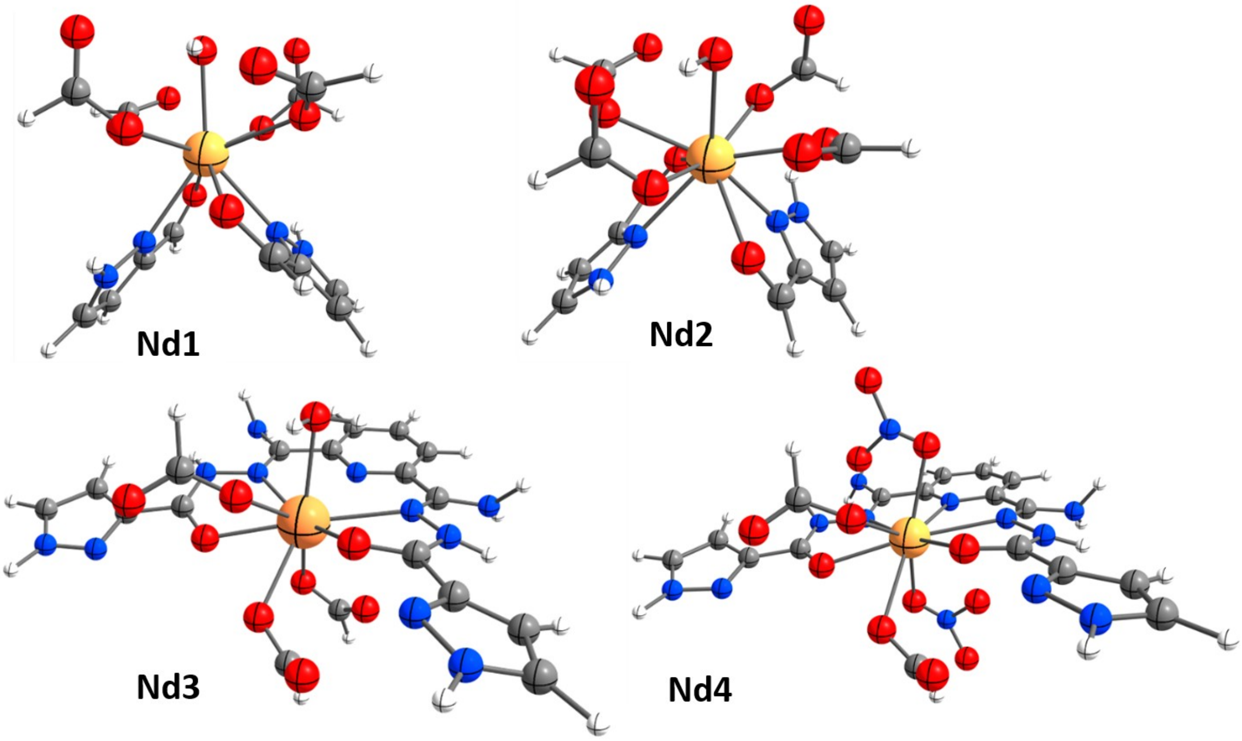

Figure S13. Monomeric models of the Nd_6 cluster. (Colour code: Orange (Nd), blue (N), red (O), grey (C) and H (white)).

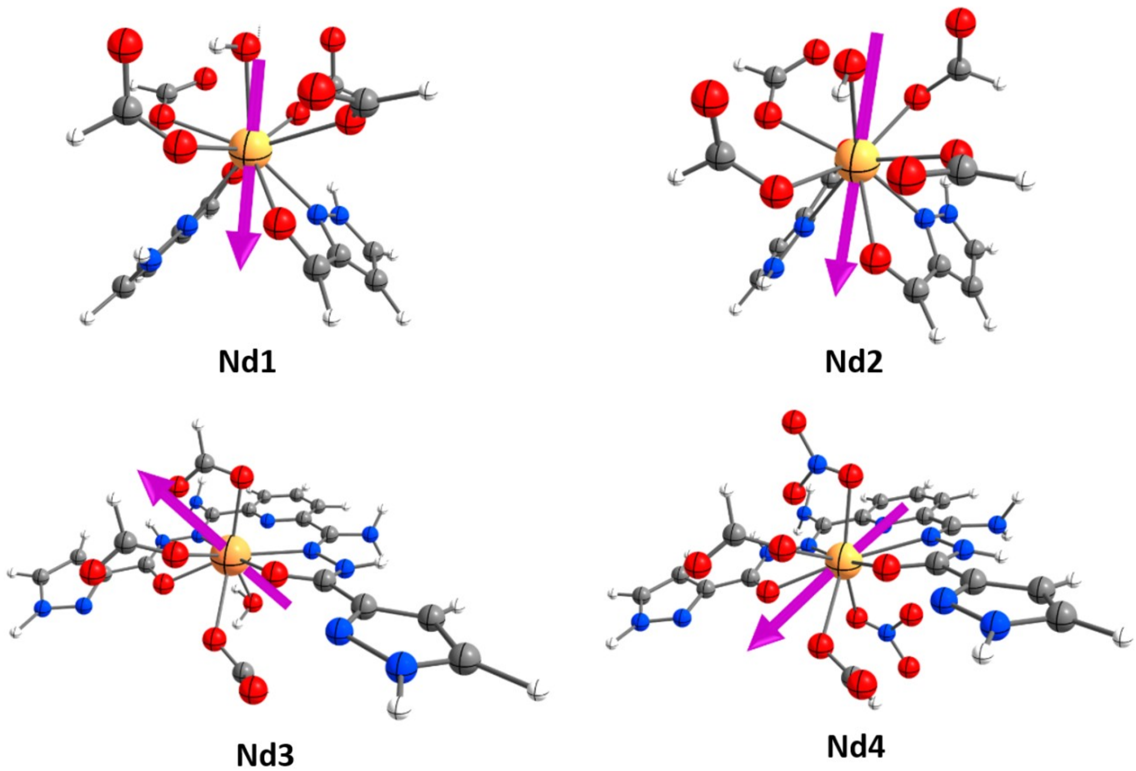

Figure S14. CASSCF+RASSI-SO computed orientation of ground state g-tensor of Nd(III) on each monomeric model. (Colour code: Orange (Nd), blue (N), red (O), grey (C) and H (white)).

Table S6. SINGLE_ANISO computed wave function decomposition analysis for all the Nd(III) centres. The major dominating values are kept in bold.

$\pm m_J$	*wave function decomposition analysis* **Nd1**
KD1	**65.8 % |±9/2⟩** + 19.6% |±5/2⟩ + 7.2% |±3/2⟩ + 5.3% |±1/2⟩
KD2	**36.2 % |±3/2⟩** + 29.8% |±5/2⟩ + 15.6% |±1/2⟩ + 9.7% |±9/2⟩
KD3	**42.8 % |±7/2⟩** + 21.6% |±3/2⟩ + 18.9% |±5/2⟩ + 9.3% |±1/2⟩
KD4	**65.6 % |±1/2⟩** + 19.1% |±3/2⟩ + 12.9% |±9/2⟩
KD5	**45.3 % |±7/2⟩** + 30.6% |±5/2⟩ + 15.7% |±3/2⟩

$\pm m_J$	*wave function decomposition analysis* **Nd2**
KD1	**64.7 % |±9/2⟩** + 16.7%|±5/2⟩ + 10.2% |±1/2⟩ +7.2% |±3/2⟩
KD2	**36.4 % |±5/2⟩** + 30.5% |±3/2⟩ + 13.3% |±9/2⟩ + 12.0% |±1/2⟩
KD3	**49.0 % |±7/2⟩** + 25.7% |±3/2⟩ + 17.7% |±5/2⟩
KD4	**30.4 % |±7/2⟩** + 29.0% |±3/2⟩ + 18.6% |±1/2⟩+ 14.5% |±3/2⟩
KD5	**54.1 % |±1/2⟩** + 14.5% |±5/2⟩ + 11.9% |±9/2⟩ + 11.8% |±7/2⟩

$\pm m_J$	*wave function decomposition analysis* **Nd3**
KD1	**45.4% |±9/2⟩**+ 21.1% |±5/2⟩ + 14.9% |±1/2⟩ + 14.0% |±7/2⟩
KD2	**33.6% |±3/2⟩** + 29.50% |±5/2⟩ + 17.8% |±9/2⟩ + 10.0% |±1/2⟩
KD3	**40.8% |±7/2⟩** + 21.3% |±1/2⟩ + 18.8% |±3/2⟩ + 10.6% |±9/2⟩
KD4	**27.9% |±5/2⟩** + 25.2% |±3/2⟩ + 24.7% |±7/2⟩ + 11.6% |±1/2⟩
KD5	**41.9% |±1/2⟩**+ 17.9% |±3/2⟩ + 15.4% |±9/2⟩ + 13.1% |±5/2⟩

$\pm m_J$	*wave function decomposition analysis* **Nd4**
KD1	**62.0% |±9/2⟩**+ 14.7% |±3/2⟩ + 14.6% |±5/2⟩
KD2	**45.1% |±5/2⟩** + 28.9% |±7/2⟩ + 12.9% |±9/2⟩
KD3	**46.4 % |±3/2⟩** + 18.0% |±1/2⟩ + 13.3% |±9/2⟩
KD4	**57.3% |±1/2⟩ +** 16.5% |±7/2⟩
KD5	**39.8% |±7/2⟩**+ 22.4% |±3/2⟩ + 21.1% |±5/2⟩

Table S7. SINGLE_ANISO computed g-tensors, and the angle of deviation from ground state g_{zz} orientation.

Nd1

Energy (cm^{-1})	g_{xx}	g_{yy}	g_{zz}	θ
0.0	0.702	1.541	4.869	0.0
114.1	0.112	0.942	4.330	21.5
194.4	0.414	1.776	3.644	67.6
342.6	0.078	0.853	5.327	50.3
364.4	0.792	2.053	3.940	72.2

Nd2

Energy (cm^{-1})	g_{xx}	g_{yy}	g_{zz}	θ
0.0	0.6425	1.7337	4.6660	0.0
107.5	1.1395	1.6824	3.0701	115.7
165.8	3.1396	2.5348	0.2080	111.4
335.6	3.1645	1.9866	0.4226	28.0
354.7	3.5485	2.2186	0.2271	144.0

Nd3

Energy (cm^{-1})	g_{xx}	g_{yy}	g_{zz}	θ
0.0	1.205	2.486	3.810	0.0
85.2	0.435	0.967	4.158	85.6
154.6	0.388	1.406	3.979	123.1
355.5	1.257	1.616	3.381	71.0
447.0	0.070	0.550	4.961	99.7

Nd4

Energy (cm^{-1})	g_{xx}	g_{yy}	g_{zz}	θ
0.0	0.902	1.794	3.959	0.0
42.0	0.793	0.844	3.738	90.3
167.6	0.006	0.854	4.397	90.2
459.6	0.123	0.315	4.856	90.2
507.0	1.511	1.548	4.459	89.8

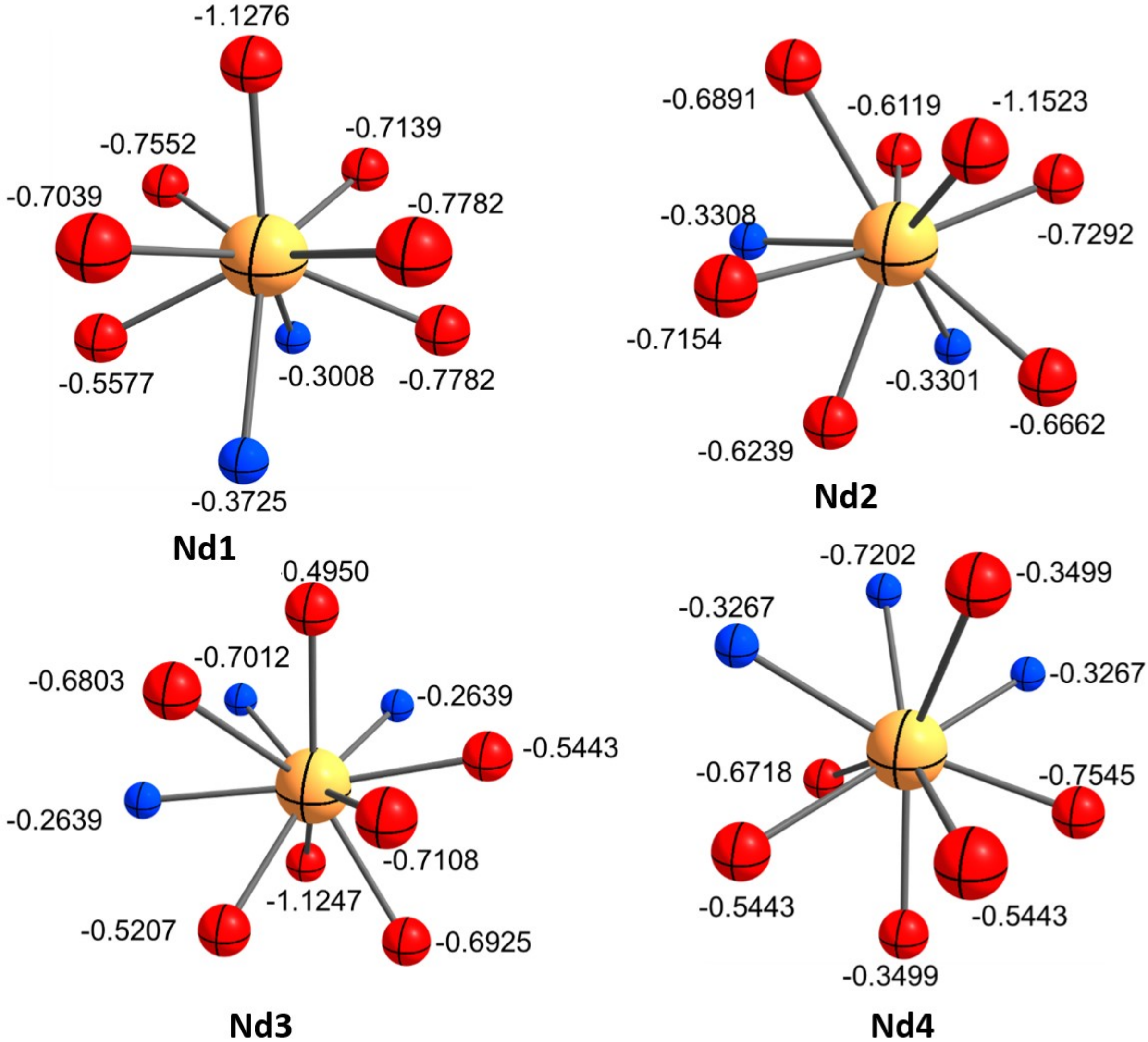

Figure S15. CASSCF computed Loprop charges on the first coordinating atoms of all unique centres.

Table S8. SINGLE_ANISO computed crystal field parameters for **Nd1** to **Nd4** centres. The CF parameters were computed using the following equation, $\hat{H}_{CF} = \sum \sum_{k=-q}^{q} B_k^q O_k^q$ and here B_k^q and O_k^q are the crystal field parameters and Steven's operator, respectively.

k	q	B_k^q	B_k^q	B_k^q	B_k^q
		Nd1	**Nd2**	**Nd3**	**Nd4**
2	-2	-8.36E-01	2.60E-01	**-1.82E+00**	7.04E-01
	-1	**-1.25E+00**	-4.52E-01	-6.38E-02	7.88E-03
	0	**-2.20E+00**	**-1.59E+00**	**-1.80E+00**	**-3.20E+00**
	1	**4.04E+00**	-5.34E-01	**-1.63E+00**	-2.69E-01
	2	8.67E-01	2.41E-01	**3.53E+00**	**5.43E+00**
4	-4	-8.14E-02	**-3.36E-02**	-3.25E-02	**-7.26E-02**
	-3	-3.49E-02	**-1.85E-02**	2.91E-02	-4.83E-03
	-2	-4.78E-03	9.75E-03	4.48E-02	8.85E-04
	-1	-1.33E-02	2.65E-03	-4.15E-03	1.69E-03
	0	-1.52E-02	-3.07E-03	8.28E-04	-7.59E-03
	1	1.63E-02	7.74E-03	6.71E-02	-4.04E-03
	2	4.58E-02	9.99E-03	2.10E-03	-1.36E-02
	3	**1.33E-01**	-3.89E-03	**-1.80E-01**	-8.51E-03
	4	-1.68E-02	7.90E-03	3.78E-02	**-1.91E-02**
6	-6	**1.05E-02**	-1.24E-03	5.02E-03	**2.41E-02**
	-5	-4.16E-03	**-2.88E-03**	**-4.21E-02**	-6.37E-05
	-4	**1.13E-02**	**2.99E-03**	**-1.60E-02**	-7.07E-03
	-3	-5.66E-03	7.39E-04	-9.63E-03	5.27E-04
	-2	-8.60E-03	1.75E-03	-2.34E-04	-8.26E-03
	-1	-1.88E-04	2.46E-04	2.88E-03	5.75E-04
	0	-1.05E-03	-2.97E-04	-4.39E-04	-1.72E-03
	1	1.51E-03	3.56E-04	**1.08E-02**	-2.01E-04
	2	7.05E-03	**-2.14E-03**	8.92E-03	**-1.87E-02**
	3	2.62E-03	**2.88E-03**	6.18E-03	-6.19E-04
	4	-7.81E-03	**3.97E-03**	-8.74E-03	**-1.34E-02**
	5	**-2.22E-02**	**-7.26E-03**	**-1.75E-02**	-6.83E-04
	6	8.31E-03	**-4.09E-03**	**-1.80E-02**	8.41E-03

Table S9. RASSI-SO computed low-lying 35 quartets (in red) and 112 doublet states (in black) along with spin-orbit coupled states (in blue, Kramer doublets) for **Nd1**. All the values are reported here in cm^{-1}.

Nd1			
0.0	14670.9	34878.1	48191.4
101.7	14684.9	34907.4	48205.5
178.4	14696.1	34928.2	48263.3
200.9	14702.3	34951.5	48288.9
265.3	14703.0	34966.5	48294.7
344.6	14737.5	35038.9	48369.4
376.3	14754.6	35063.1	60933.9
499.4	14758.9	35133.6	60948.8
520.9	14762.8	35137.3	61043.9
537.4	14780.0	35193.5	61108.3
568.7	14784.0	35201.1	61205.0
798.1	19270.9	35283.4	61222.0
820.6	19279.9	35288.3	61281.0
14621.7	19326.6	35472.5	61362.8
14655.9	19343.6	35478.0	61368.3
14723.9	19368.1	35627.8	86899.3
14822.1	19412.1	35638.4	87049.9
14827.7	19421.0	35770.5	87251.1
14915.0	19503.4	35791.2	87431.1
14942.4	19517.1	35882.7	87572.3
15043.3	21512.1	35899.4	87733.4
22823.6	21512.4	35956.8	87833.2
22874.4	21713.8	35989.3	
22969.2	21716.6	36013.5	
23005.6	21823.9	36070.1	
23038.9	21824.6	36075.6	
23119.2	21896.9	36264.5	
23150.8	21904.7	36265.1	
23268.4	21933.0	39741.1	
23365.5	21947.2	39760.0	
37167.9	21952.8	39843.9	
37306.2	22002.3	39883.3	
37514.2	22003.2	39903.2	
37640.3	22144.2	39997.8	
37818.5	22144.4	40014.0	
	26375.2	40061.1	
	26387.7	40070.7	
	26433.5	40131.5	
	26492.7	40143.4	
	26732.0	40752.4	
	26744.3	40862.8	
	26756.9	41029.4	
	26764.1	41105.4	
	34720.6	41153.0	

	34733.7	48116.8	

0.0	19315.7	30421.9	44297.6
114.1	19327.0	32897.7	44364.4
194.4	19352.8	33156.7	44428.0
342.6	21989.6	37376.0	44509.1
364.4	22034.5	37513.8	44543.6
2042.5	22080.6	37572.8	44604.1
2135.4	22143.9	37655.8	45822.0
2168.1	23777.7	37781.2	45953.1
2196.8	23885.8	37851.6	45993.2
2239.4	23963.8	37996.6	51157.5
2253.8	23981.3	38213.5	51296.1
4135.1	23997.4	38374.5	51353.4
4234.7	24089.1	38516.5	53004.9
4265.1	24163.5	38614.5	53085.0
4297.3	24198.0	38629.5	53119.3
4338.8	24242.5	38689.2	53146.4
4372.9	24382.0	38748.1	64028.5
4427.7	24743.1	38766.2	64135.9
6254.0	24804.2	38810.4	64254.4
6375.0	24844.2	38860.0	64335.9
6433.0	24923.4	38941.5	64427.9
6519.7	24972.7	38963.3	65008.5
6564.7	25409.9	39023.1	65173.6
6624.7	25435.3	39064.4	65318.8
6746.8	25492.0	39084.7	65437.6
6837.4	25588.0	39151.2	90000.4
15789.8	25927.3	39378.4	90284.2
15882.1	26114.9	39533.2	90520.2
15928.9	26218.1	39617.8	90755.4
15961.7	26292.5	39679.0	91487.4
16037.9	26342.7	39844.9	91872.0
16071.7	26373.4	39868.1	92172.2
16107.9	26436.3	40019.2	
16869.8	26548.5	40160.5	
16923.5	26982.2	40266.9	
16996.7	27012.3	40342.7	
17820.9	27061.8	40398.8	
17857.5	27115.6	40470.6	
17866.7	27166.5	40650.3	
17890.9	27686.9	41504.1	
17970.4	27794.1	41697.2	
18064.7	28361.5	41850.9	
18962.9	28420.1	41970.7	
19014.2	28450.5	42990.5	
19078.0	28489.9	43092.2	
19121.0	28564.3	43189.0	

19188.6	28639.7	43264.1	
19251.2	29873.4	43331.8	
19257.1	30097.4	44175.9	
19290.1	30226.2	44207.5	

Table S10. RASSI-SO computed low-lying 35 quartets (in red) and 112 doublet states (in black) along with spin-orbit coupled states (in blue, Kramer doublets) for **Nd2**. All the values are reported here in cm^{-1}.

Nd2			
0.0	14684.8	34888.7	48182.7
103.9	14694.2	34899.8	48217.9
175.5	14705.1	34957.0	48263.8
243.7	14714.7	34974.4	48290.7
263.7	14716.4	35017.1	48309.0
342.2	14744.7	35050.9	48360.2
396.9	14753.5	35059.4	60941.0
474.0	14758.8	35133.3	60965.7
505.1	14760.4	35141.8	61075.8
567.4	14781.5	35160.2	61137.8
571.8	14783.3	35167.7	61176.6
807.9	19299.9	35327.0	61238.3
829.5	19309.4	35329.4	61272.8
14633.9	19331.4	35463.9	61325.5
14715.9	19354.8	35469.9	61341.5
14732.5	19368.7	35628.5	86967.9
14793.3	19419.1	35637.6	87078.4
14828.3	19420.9	35777.8	87260.5
14896.2	19497.1	35807.3	87457.8
14954.7	19517.2	35911.4	87588.5
15043.1	21564.1	35919.2	87681.5
22793.9	21564.9	35973.1	87722.7
22930.4	21713.3	35994.5	
22961.3	21716.4	36008.1	
23036.4	21822.5	36054.5	
23086.6	21823.6	36061.8	
23118.2	21896.2	36137.1	
23139.3	21909.9	36138.9	
23238.8	21955.4	39777.3	
23337.3	21960.0	39789.2	
37193.8	21984.8	39830.3	
37328.0	22035.7	39861.7	
37541.2	22043.0	39922.2	
37641.1	22048.1	39998.0	
37752.5	22051.3	40023.8	
	26401.0	40047.1	
	26433.4	40076.9	
	26440.8	40111.5	
	26513.7	40119.3	
	26723.3	40770.0	
	26733.3	40891.9	
	26740.5	41054.1	

	26742.9	41076.0	
	34818.9	41124.7	
	34825.9	48114.3	

0.0	19299.7	30391.7	44265.9
107.5	19312.4	32903.8	44366.2
165.8	19333.1	33129.5	44410.5
335.6	21996.8	37428.8	44488.2
354.7	22026.1	37516.5	44522.9
2047.0	22067.7	37596.7	44574.1
2127.8	22128.9	37655.7	45815.9
2157.9	23811.7	37757.8	45940.4
2175.7	23889.1	37791.7	45966.5
2226.1	23948.7	38035.3	51150.0
2240.2	23961.4	38182.8	51282.0
4140.9	23978.1	38360.3	51332.6
4234.6	24076.4	38517.7	52994.6
4248.2	24155.9	38621.9	53064.1
4285.7	24204.9	38676.7	53108.5
4307.2	24263.9	38689.2	53129.8
4363.3	24285.9	38736.7	64023.8
4419.5	24740.4	38749.9	64147.7
6252.6	24786.9	38817.4	64235.3
6370.6	24839.5	38824.1	64319.5
6421.7	24926.0	38888.1	64379.1
6505.3	24949.3	38931.0	65007.4
6543.6	25398.2	39001.3	65186.1
6610.8	25419.6	39020.3	65293.6
6740.4	25488.4	39069.9	65389.0
6829.1	25568.5	39145.2	90034.8
15792.3	25958.1	39378.1	90282.7
15879.3	26109.9	39533.1	90526.6
15910.4	26205.5	39573.2	90659.5
15947.4	26280.6	39715.7	91509.9
16028.4	26341.5	39822.0	91876.2
16049.2	26384.9	39851.1	92079.5
16110.0	26436.1	40010.6	
16875.2	26446.3	40158.1	
16905.6	26973.9	40274.5	
16979.2	26995.3	40343.9	
17828.4	27061.8	40381.4	
17848.6	27098.2	40433.5	
17856.7	27139.5	40508.8	
17868.8	27686.0	41506.6	
17964.9	27779.0	41701.0	
18045.4	28369.5	41834.0	
18978.2	28400.5	41917.7	
19005.3	28450.8	43003.7	

19054.7	28487.6	43066.1	
19116.1	28538.9	43187.3	
19161.1	28598.6	43255.9	
19243.0	29866.0	43289.6	
19254.1	30114.1	44178.3	
19286.6	30201.2	44207.1	

Table S11. RASSI-SO computed low-lying 35 quartets (in red) and 112 doublet states (in black) along with spin-orbit coupled states (in blue, Kramer doublets) for **Nd3**. All the values are reported here in cm^{-1}.

Nd3			
0.0	14672.8	34721.5	48250.2
58.4	14675.1	34785.4	48323.9
92.6	14691.7	34845.1	48338.8
127.8	14699.0	34954.9	48383.7
193.2	14735.0	34970.2	48415.5
286.0	14741.3	35097.1	48442.1
392.1	14763.0	35102.5	60984.2
512.7	14776.1	35236.6	61038.1
556.3	14781.8	35242.2	61119.1
622.4	14824.2	35381.3	61162.0
676.6	14837.9	35383.2	61214.9
897.7	19253.8	35487.7	61344.1
919.9	19267.1	35489.3	61403.4
14551.6	19347.0	35612.1	61551.4
14665.1	19353.4	35615.3	61568.6
14730.1	19431.0	35651.2	86923.7
14853.0	19456.1	35678.0	87129.7
14874.7	19500.6	35729.3	87237.0
14969.1	19550.8	35759.0	87559.3
15026.9	19572.6	35803.2	87684.1
15108.7	21623.2	35895.9	88063.9
22718.2	21625.8	35911.2	88159.4
22895.5	21703.0	36056.6	
23034.6	21711.9	36064.0	
23093.8	21743.3	36240.9	
23148.6	21774.7	36243.2	
23167.4	21792.2	36523.7	
23239.8	21849.1	36523.7	
23284.1	21857.3	39768.8	
23429.5	21956.6	39800.8	
37163.1	21960.3	39868.8	
37342.5	22115.9	39898.3	
37526.4	22117.8	39989.8	
37841.8	22365.2	40080.0	
37902.8	22366.1	40091.4	
	26356.7	40154.1	
	26359.5	40171.1	
	26471.7	40245.1	
	26480.7	40258.7	
	26823.1	40839.1	

26830.1	40906.7
26841.2	40993.9
26854.8	41246.0
34603.4	41311.4
34619.9	48159.3

0.0	19343.9	30500.1	44322.5
85.2	19385.3	32905.8	44468.1
154.6	19407.2	33245.3	44502.2
355.5	21995.3	37283.4	44588.9
447.0	22062.3	37426.6	44645.5
2079.1	22141.2	37561.2	44745.5
2111.3	22207.8	37724.2	45922.5
2154.5	23888.5	37890.6	46012.2
2192.7	23926.7	38028.3	46105.5
2251.5	23960.5	38181.3	51255.2
2338.4	23995.5	38296.8	51325.0
4169.6	24021.3	38356.8	51490.5
4205.2	24063.4	38452.3	53104.7
4256.3	24097.1	38567.7	53154.3
4281.9	24197.7	38582.9	53212.8
4364.1	24349.5	38685.3	53261.1
4424.2	24588.9	38740.5	64106.9
4500.6	24784.6	38787.5	64218.4
6259.9	24825.2	38900.7	64307.6
6330.1	24855.5	38927.6	64468.3
6416.7	24980.1	39013.2	64622.2
6465.1	25065.6	39116.9	65084.5
6636.2	25428.9	39144.9	65233.1
6709.9	25489.5	39183.9	65426.9
6813.0	25563.0	39243.3	65641.4
6931.8	25656.1	39278.9	90060.0
15782.4	26032.4	39436.0	90326.0
15902.5	26125.4	39640.9	90650.8
15941.6	26172.3	39688.8	91082.7
16007.4	26219.7	39854.6	91546.6
16032.9	26293.0	39945.6	91972.0
16103.2	26407.5	39967.8	92499.4
16184.4	26567.4	40029.4	
16854.8	26779.2	40114.5	
16992.3	26980.2	40217.3	
17035.0	27069.3	40342.0	
17792.7	27141.2	40490.8	
17894.8	27174.5	40676.8	
17906.6	27217.3	40943.6	
17940.7	27717.8	41563.9	
18036.5	27859.7	41727.3	
18118.4	28393.7	41910.9	

18944.2	28454.9	42138.0	
19030.8	28541.2	43042.8	
19129.3	28569.1	43121.3	
19182.3	28642.6	43272.0	
19235.8	28679.8	43358.5	
19260.4	29926.6	43465.1	
19289.6	30057.8	44225.2	
19307.6	30351.6	44269.0	

Table S12. RASSI-SO computed low-lying 35 quartets (in red) and 112 doublet states (in black) along with spin-orbit coupled states (in blue, Kramer doublets) for **Nd4**. All the values are reported here in cm^{-1}.

	Nd4		
0.0	14766.1	34703.8	48270.7
38.0	14769.6	34789.3	48413.9
53.6	14787.7	34792.3	48437.2
144.4	14789.9	34919.0	48481.3
352.8	14804.9	34919.1	48513.6
397.9	14806.5	34981.4	48543.7
453.1	14819.6	34987.0	60967.3
595.6	14821.8	35261.2	61016.7
644.9	14839.2	35265.0	61110.9
741.2	14875.2	35313.3	61264.3
872.8	14910.8	35326.6	61306.2
1084.3	19263.4	35400.8	61353.6
1173.3	19275.8	35422.9	61504.7
14463.7	19453.2	35583.2	61739.5
14809.8	19459.8	35619.7	61752.7
14865.0	19552.7	35761.3	86772.0
14940.4	19574.4	35808.7	87076.1
15000.5	19594.5	35929.3	87285.4
15011.0	19682.0	35948.1	87596.7
15031.2	19696.4	36028.9	87617.7
15329.6	21482.0	36044.5	88222.8
22750.6	21489.1	36182.6	88587.5
23003.9	21664.0	36249.7	
23091.4	21676.5	36261.2	
23137.6	21841.8	36521.5	
23181.0	21889.6	36553.4	
23339.9	21896.2	36780.8	
23340.9	21965.8	36789.2	
23451.8	22014.7	39823.1	
23527.3	22139.2	39846.6	
37203.7	22153.1	39859.3	
37298.0	22300.3	39906.7	
37522.9	22324.3	40086.9	
38080.1	22463.6	40114.1	
38111.3	22465.6	40150.2	
	26343.7	40317.6	
	26355.4	40323.7	
	26474.4	40378.5	

	26492.4	40424.7	
	26971.8	40779.9	
	26981.9	40991.0	
	26997.6	41213.2	
	27030.1	41378.8	
	34610.8	41387.5	
	34644.4	48232.5	

0.0	19373.9	30390.3	44214.8
42.0	19411.8	30627.8	44312.0
167.6	19456.9	32859.8	44510.5
459.6	21969.6	33319.8	44531.5
507.0	22129.1	37252.0	44621.0
2054.1	22192.9	37377.1	44795.1
2102.6	22256.1	37477.8	44814.8
2191.1	23702.7	37583.9	45904.5
2292.7	23893.5	37808.6	46106.6
2330.6	23977.2	37931.0	46140.1
2381.7	24009.1	38093.9	51227.6
4141.9	24079.1	38216.3	51416.5
4185.1	24088.9	38447.8	51495.5
4268.6	24150.8	38526.3	53114.1
4386.4	24304.6	38587.3	53184.4
4423.7	24495.8	38641.7	53259.8
4502.7	24649.1	38685.7	53289.3
4565.5	24774.3	38736.5	64038.6
6212.0	24820.0	38795.1	64183.7
6269.5	24928.4	38879.6	64328.0
6458.1	25069.7	38936.9	64493.9
6549.0	25085.2	39075.1	64745.4
6646.4	25424.4	39115.7	65002.2
6782.9	25529.7	39166.7	65263.1
6967.7	25608.0	39190.7	65406.4
7038.5	25720.3	39348.6	65781.6
15755.1	25841.5	39404.6	89894.4
15911.5	26027.8	39440.8	90269.7
15929.9	26181.6	39628.6	90616.3
16054.3	26285.2	39680.2	91285.3
16083.6	26394.8	39738.3	91420.1
16153.3	26394.8	39829.0	91917.5
16212.7	26531.8	40047.1	92747.9
16834.5	26681.4	40074.0	
17021.0	26824.1	40230.3	
17097.4	26999.3	40308.8	
17774.2	27047.5	40458.0	
17924.9	27184.2	40631.6	
17940.5	27220.1	40916.7	
17973.5	27269.9	41137.7	

18048.5	27726.7	41486.9
18202.1	27902.2	41756.7
18898.2	28431.0	41974.6
19069.9	28500.5	42293.8
19142.9	28560.6	43029.6
19226.2	28627.9	43103.7
19268.3	28674.7	43264.1
19296.7	28727.4	43434.1
19323.1	29911.3	43566.7
19334.8	30037.1	44192.0

References:

1. Alvarez, S.; Alemany, P.; Casanova, D.; Cirera, J.; Llunell, M.; Avnir, D. Shape maps and polyhedral interconversion paths in transition metal chemistry, *Coord. Chem. Rev*. **2005**, *249*, 1693-1708, 112.

2. Casanova, D.; Llunell, M.; Alemany, P.; Alvarez, S. The Rich Stereochemistry of Eight-Vertex Polyhedra: A Continuous Shape Measures Study, *Chem. Eur. J.* **2005**, *11*, 1479- 1494.